

## Article

# A Decadal Change in Atmospheric Nitrogen Deposition at a Rural Site in Southern China

Kaige Ren <sup>1,†</sup>, Yalan Zhou <sup>1,†</sup> , Jiarui Liu <sup>2</sup>, Ziyin Yu <sup>1</sup>, Xin Ma <sup>1</sup>, Ruotong Si <sup>1</sup>, Zhang Wen <sup>1</sup>, Wen Xu <sup>1</sup>, Aohan Tang <sup>1</sup>, Jianlin Shen <sup>3</sup>, Keith Goulding <sup>4</sup>  and Xuejun Liu <sup>1,\*</sup> 

<sup>1</sup> State Key Laboratory of Nutrient Use and Management, College of Resources and Environmental Sciences, National Academy of Green Agriculture Development, China Agricultural University, Beijing 100193, China; rkg@cau.edu.cn (K.R.); zhoyalan@cau.edu.cn (Y.Z.); s20223030425@cau.edu.cn (Z.Y.); maxin@cau.edu.cn (X.M.); ruotong1231@cau.edu.cn (R.S.); wenzhang@caep.org.cn (Z.W.); wenxu@cau.edu.cn (W.X.); aohantang@cau.edu.cn (A.T.)

<sup>2</sup> Yali Middle School, Changsha 410007, China; s20233030447@cau.edu.cn

<sup>3</sup> Institute of Subtropical Agriculture, Chinese Academy of Sciences, Changsha 410125, China; jlshen@isa.ac.cn

<sup>4</sup> Rothamsted Research, Harpenden AL5 2JQ, UK; keith.goulding@rothamsted.ac.uk

\* Correspondence: liu310@cau.edu.cn

† These authors contributed equally to this work.

**Abstract:** Elevated atmospheric reactive nitrogen (Nr) emissions and the subsequent nitrogen (N) deposition have negatively impacted the global environment, particularly in China. In order to assess the long-term trends in atmospheric N deposition in the south of China, Taojiang County in Hunan Province was selected as a representative rural area for study. We analyzed interannual variation in atmospheric Nr, including gaseous ammonia (NH<sub>3</sub>), nitrogen dioxide (NO<sub>2</sub>), nitrate acid (HNO<sub>3</sub>) vapor, particulate ammonium (NH<sub>4</sub><sup>+</sup>), and nitrate (NO<sub>3</sub><sup>-</sup>) in air and NH<sub>4</sub><sup>+</sup>-N and NO<sub>3</sub><sup>-</sup>-N in precipitation from 2011 to 2020. The 10-year average atmospheric wet-plus-dry N deposition was 41.9 kg N ha<sup>-1</sup> yr<sup>-1</sup>, which decreased by approximately 24% after 2012, indicating that NH<sub>3</sub> and NO<sub>x</sub> emissions were effectively reduced by emission controls introduced in 2013. Wet deposition accounted for approximately 74% of the total N deposition and was significantly influenced by annual precipitation amount. Reduced N (NH<sub>3</sub>, pNH<sub>4</sub><sup>+</sup>, and NH<sub>4</sub><sup>+</sup> in rainwater) was the dominant form, comprising approximately 58% of the total N deposition, while oxidized N (pNO<sub>3</sub><sup>-</sup>, NO<sub>2</sub>, HNO<sub>3</sub>, and NO<sub>3</sub><sup>-</sup> in rainwater) accounted for 42% of the total N deposition. Atmospheric HNO<sub>3</sub>, NO<sub>2</sub>, and NH<sub>3</sub> concentrations and deposition declined by 30–80% over the decade, while particulate NH<sub>4</sub><sup>+</sup> and NO<sub>3</sub><sup>-</sup> concentrations and deposition remained at relatively stable levels, which suggests that ongoing research and policy should focus on rural particulate pollution. Future strategies must concentrate on the integrated control of NH<sub>3</sub> and NO<sub>x</sub> emissions to mitigate air pollution and protect human health, particularly in rural areas because current abatement efforts are primarily directed toward urban areas and the industrial sector, whereas non-point source NH<sub>3</sub> pollution, influenced mainly by agricultural activities, dominates in rural regions.

**Keywords:** atmospheric reactive nitrogen; wet and dry deposition; temporal variation; pollution control; ammonia abatement



**Citation:** Ren, K.; Zhou, Y.; Liu, J.; Yu, Z.; Ma, X.; Si, R.; Wen, Z.; Xu, W.; Tang, A.; Shen, J.; et al. A Decadal Change in Atmospheric Nitrogen Deposition at a Rural Site in Southern China. *Atmosphere* **2024**, *15*, 583. <https://doi.org/10.3390/atmos15050583>

Academic Editor: Laszlo Bencs

Received: 18 February 2024

Revised: 27 April 2024

Accepted: 6 May 2024

Published: 10 May 2024



**Copyright:** © 2024 by the authors. Licensee MDPI, Basel, Switzerland. This article is an open access article distributed under the terms and conditions of the Creative Commons Attribution (CC BY) license (<https://creativecommons.org/licenses/by/4.0/>).

## 1. Introduction

Atmospheric reactive nitrogen (Nr) emissions have been increasing every year, caused by rapid economic development and the increasing global population [1]. Anthropogenic activities are the main contributors to this increase in Nr deposition [2], with ammonia (NH<sub>3</sub>) and nitrogen oxides (NO<sub>x</sub>) being the main sources of nitrogen (N) emissions [3]. Although there are some urban sources from fossil fuel combustion [4–6], NH<sub>3</sub> mainly originates from agricultural activities such as livestock farming and fertilizer application [7,8], while NO<sub>x</sub> is mainly derived from fossil fuel combustion such as industrial and

traffic emissions [9]. Human-induced pollutant emissions dominate  $N_r$  emissions [10] and deposition [2], damaging the Earth's ecosystems (e.g., reducing biodiversity) and triggering a series of ecological and environmental problems [11,12]. Therefore, reducing  $NH_3$  and  $NO_x$  emissions is essential for reducing N deposition for realizing a green eco-environment [13]. In recent years,  $NO_x$  (and sulfur dioxide ( $SO_2$ )) emissions have been effectively controlled in China and in other countries, and so the focus on  $NH_3$  reduction has gradually increased [14]. Some research has reported long-term trends in wet/bulk and dry N deposition in north China [15,16], revealing different responses of N deposition to changes in  $N_r$  emissions. However, to date, no systematic studies have reported recent interannual changes in N deposition in the rural areas of southern China.

Hunan Province is a major agricultural region in southern China, with a high rate of N fertilizer use and intensive livestock (especially pig) production. As a consequence, high  $NH_3$  and  $NO_x$  emissions and N deposition have been observed [17]. Local agricultural production methods have changed greatly since the 2000s, with the traditional double rice cropping system gradually being replaced by single rice production, with decreased overall N fertilizer use. However, pig (as a typical livestock) production has been transformed from small scale, family-based systems to a more efficient, larger scale and no longer family-based systems with spatial relocation [18]. This transformation of both crop and livestock production may have reduced  $NH_3$  emissions. In addition, farmers now use natural gas instead of wood and/or crop straw as fuel, which could lead to a reduction in  $NO_x$  emissions and consequently of particulate matter pollution in rural regions of southern China. We therefore quantified the decadal changes of wet/bulk and dry N deposition at a rural deposition monitoring site in Taojiang County, Hunan Province, from 2011 to 2020. Our hypothesis is that atmospheric N deposition will have decreased substantially due to the reduction in both  $NH_3$  and  $NO_x$  emissions associated with agricultural production transformations and energy structural changes in this region. Moreover, the change in agricultural production styles could be the main driving factor of atmospheric N deposition locally and regionally [1,2,19]. Our research aims to guide the more comprehensive and effective control of  $N_r$  emissions and pollution.

## 2. Materials and Methods

### 2.1. Study Sites

The study area is located in the north–central part of Taojiang County, Hunan Province, in southern China, which belongs to the subtropical monsoon humid climate zone, with a 1990–2010 average annual temperature of 16.6 °C and an average annual precipitation of 1700 mm. The monitoring sampling site was at Songmudian Village (111.97° E, 28.61° N) in Wujishan Township, Taojiang County, which is a typical rural site (Figure 1). The sampling site is located at the edge of hills and surrounded by rice fields, ensuring the adequate collection of atmospheric deposition samples. Paddy rice, including early, middle, and/or late rice (sown in mid-March, mid-May, and late June, respectively), is the major local crop. Double rice (early rice and late rice) was the traditional cropping system, but now more and more farmers plant only a single crop of rice. Fertilizer application is mostly based on compound fertilizers and urea, with the compound fertilizer applied at planting and urea 7–10 days later. The development of local animal husbandry has been slow, with a small number of farmers breeding crossbred yellow cows, black goats, and pigs, and the resultant manure is generally used on farmland or in biogas digesters. Dry and wet N deposition was sampled and quantified from January 2011 to December 2020.

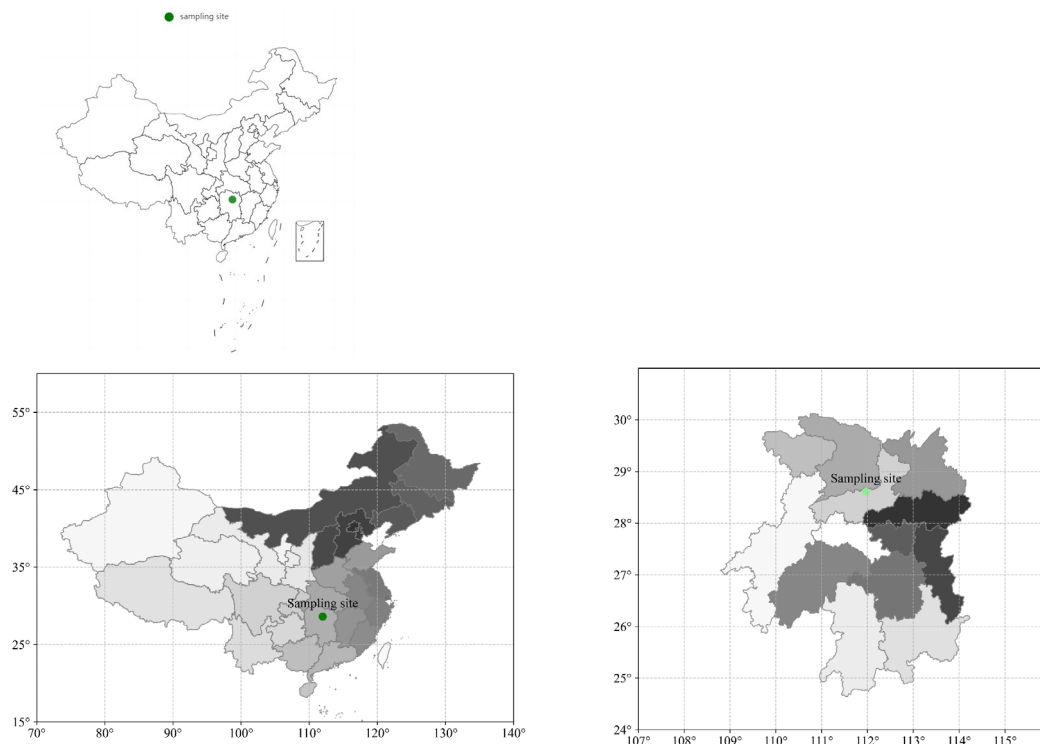


**Figure 1.** Map showing the monitoring site at Taojiang County, Hunan Province, China.

## 2.2. Sample Collection and Data Analysis

Gaseous  $\text{NH}_3$ ,  $\text{NO}_2$ ,  $\text{HNO}_3$ , particulate ammonium, and particulate nitrate ( $\text{pNH}_4^+$  and  $\text{pNO}_3^-$ ) samples were collected monthly using ALPHA samplers ( $\text{NH}_3$ , Adapted Low-cost High Absorption, Center for Ecology and Hydrology, Edinburgh, UK), Gradko diffusion tubes ( $\text{NO}_2$ , Gradko International Limited, London, UK), and a DELTA system ( $\text{HNO}_3$ ,  $\text{pNH}_4^+$  and  $\text{pNO}_3^-$ , Denuder for Long-Term Atmospheric sampling, Center for Ecology and Hydrology, Edinburgh, UK), and their monthly mean concentrations (in units of  $\mu\text{g N m}^{-3}$ ) measured with a Continuous Flow Analyzer (AA3, Bran + Luebbe GmbH, Norderstedt, Germany, for all Nr species except  $\text{NO}_2$ ) and a colorimetric method by absorption at a wavelength of 542 nm for  $\text{NO}_2$ , respectively. Dry deposition velocities of five Nr species were simulated using the global atmospheric chemistry transport model GEOS-Chem (<http://geos-chem.org>, accessed on 31 January 2021, provided by Dr. Zhang Lin at Peking University). Based on the influential method, the monthly dry deposition of Nr components can be estimated by multiplying the measured atmospheric Nr concentrations by the corresponding simulated dry deposition velocities [14].

Rain and snow samples were automatically collected using a rain gauge (SDM6, Tianjin Weather Equipment Inc., Tianjin, China), and the precipitation amount was recorded in mm. The annual precipitation (sum of rainfall and snowfall) from 2011 to 2020 is shown in Table 1. The samples were subjected to appropriate pre-treatment, and later measured using the Continuous Flow Analyzer (as mentioned earlier), which was calibrated to derive the inorganic N concentrations in the precipitation, i.e., the concentrations of  $\text{NH}_4^+\text{-N}$  and  $\text{NO}_3^-\text{-N}$  in  $\text{mg N L}^{-1}$ . Wet deposition of atmospheric Nr fractions was then obtained by multiplying their concentrations in precipitation by the precipitation amount. Excel was used for the preliminary processing of the data and correlation analysis. Graphs were plotted using Python and Origin 2023b software.

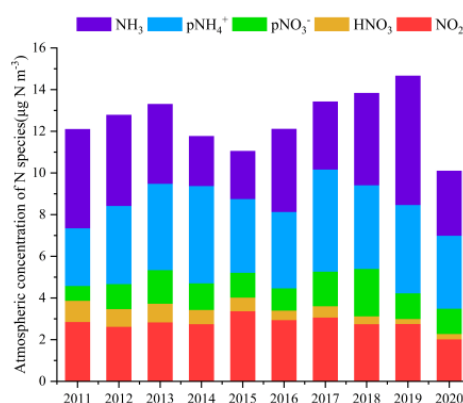
**Table 1.** Annual precipitation (mm) at the monitoring site in southern China from 2011 to 2020.

Year	2011	2012	2013	2014	2015	2016	2017	2018	2019	2020
Precipitation	753.2	1740.9	1106.3	1399.6	1461.1	1826.7	1521.7	1398.1	1286.8	1608.2

### 3. Results

#### 3.1. Temporal Variation in Atmospheric Nr Components

Annual mean concentrations of gaseous  $\text{NH}_3$ ,  $\text{HNO}_3$ , and  $\text{NO}_2$  as well as particulate  $\text{NH}_4^+$  ( $\text{pNH}_4^+$ ) and  $\text{NO}_3^-$  ( $\text{pNO}_3^-$ ) are shown in Figure 2. The annual mean  $\text{NH}_3$  concentration ranged from 2.29 to  $6.19 \mu\text{g N m}^{-3}$ , with a mean value of  $3.85 \mu\text{g N m}^{-3}$ , and showed a general decline from 2011 to 2015, with the lowest value occurring in 2015, followed by an increase up to 2019, when the maximum increase and the highest concentration ( $6.19 \mu\text{g N m}^{-3}$ ) was measured, after which the 2020 mean concentration decreased to  $3.11 \mu\text{g N m}^{-3}$ , less than the mean value in 2011. The annual mean  $\text{pNH}_4^+$  concentration ranged from 2.77 to  $4.90 \mu\text{g N m}^{-3}$  with a mean value of  $3.92 \mu\text{g N m}^{-3}$ , and the lowest and highest values occurred in 2011 and 2017, respectively. Excluding 2011, the  $\text{pNH}_4^+$  concentration did not show significant changes regardless of some turbulence during the 10-year period. The annual mean  $\text{HNO}_3$  vapor concentrations were in the range of  $0.24\text{--}1.02 \mu\text{g N m}^{-3}$  with a mean value of  $0.60 \mu\text{g N m}^{-3}$ . The mean  $\text{HNO}_3$  concentration in 2020 was 74.6% lower than that in 2011 ( $0.76 \mu\text{g N m}^{-3}$ ). Annual mean  $\text{pNO}_3^-$  concentrations were in the range of  $0.71\text{--}2.28 \mu\text{g N m}^{-3}$  with a mean value of  $1.34 \mu\text{g N m}^{-3}$ , with the lowest and highest concentrations occurring in 2011 and 2018, respectively. In general,  $\text{pNO}_3^-$  concentrations increased gradually from 2011 to 2018 but decreased after 2018. The annual mean concentrations of gaseous  $\text{NO}_2$  ranged from 2.02 to  $3.37 \mu\text{g N m}^{-3}$ , with a mean value of  $2.80 \mu\text{g N m}^{-3}$ . The annual mean  $\text{NO}_2$  concentration was relatively stable except in 2020, when the lowest concentration was observed. From 2011 to 2020, the total annual mean concentrations of reduced N ( $\text{NH}_x$ , sum of  $\text{NH}_3 + \text{pNH}_4^+$ ) varied between 5.83 and  $10.43 \mu\text{g N m}^{-3}$  and decreased until 2015, then increased to the highest value in 2019, followed by a rapid decrease of 36.7% in 2020. Total annual mean oxidized N ( $\text{NO}_y$ , sum of  $\text{HNO}_3 + \text{NO}_2 + \text{pNO}_3^-$ ) concentrations ranged from 3.49 to  $5.40 \mu\text{g N m}^{-3}$  and showed relatively little variation during the research period, with the highest concentration in 2018 and the lowest concentration in 2020. The  $\text{NO}_y$  concentration in 2020 was 23.8% lower than that in 2011.

**Figure 2.** Distribution of annual mean concentrations of atmospheric Nr components for the period 2011–2020.

#### 3.2. Changes in Monthly Mean Atmospheric Nr Concentrations

The monthly mean  $\text{NH}_3$  concentrations ( $1.29\text{--}7.41 \mu\text{g N m}^{-3}$ ) averaged  $3.52 \mu\text{g N m}^{-3}$  and showed distinct seasonal variations, with the highest concentration in summer and the lowest mostly in winter (Figure 3). Monthly mean  $\text{pNH}_4^+$  concentrations ranged from 1.95 to  $5.49 \mu\text{g N m}^{-3}$  with a mean value of  $3.69 \mu\text{g N m}^{-3}$ , with most of the highest

values occurring in spring and the lowest in summer. The monthly mean  $\text{HNO}_3$  vapor concentrations were in the range of  $0.43\text{--}0.74 \mu\text{g N m}^{-3}$  with a mean value of  $0.57 \mu\text{g N m}^{-3}$ . The seasonal variation in  $\text{HNO}_3$  concentration was relatively small, with the highest concentrations in spring and winter. Monthly mean  $\text{pNO}_3^-$  concentrations were in the range of  $0.50\text{--}2.58 \mu\text{g N m}^{-3}$  with a mean value of  $1.26 \mu\text{g N m}^{-3}$ ; the concentration was high in spring and winter and low in summer and autumn. The monthly mean concentrations of gaseous  $\text{NO}_2$  ranged from  $1.58$  to  $3.88 \mu\text{g N m}^{-3}$ , with a mean value of  $2.60 \mu\text{g N m}^{-3}$ . The seasonal concentration changes are similar to those of  $\text{pNO}_3^-$ , with the highest concentrations in spring and winter and the lowest in summer and autumn.

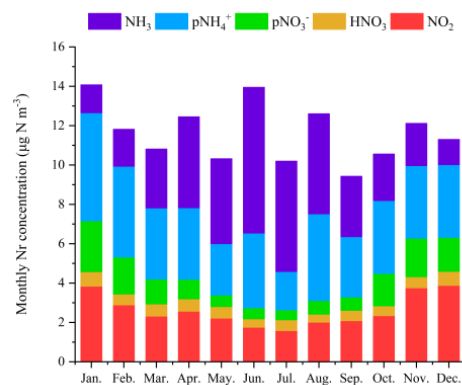


**Figure 3.** Mean monthly distribution of mean atmospheric Nr concentrations for the period 2011–2020.

### 3.3. Changes in Annual Mean Dry N Deposition

The annual mean deposition of gaseous  $\text{NH}_3$ ,  $\text{HNO}_3$ , and  $\text{NO}_2$  and particulate  $\text{pNH}_4^+$  and  $\text{pNO}_3^-$  was in the ranges of  $3.10\text{--}7.93$ ,  $0.74\text{--}4.04$ ,  $1.06\text{--}1.75$ ,  $1.30\text{--}2.36$ , and  $0.40\text{--}0.78 \text{ kg N ha}^{-1}$ , respectively, over the 10 years. The annual mean deposition of  $\text{NO}_2$  and  $\text{HNO}_3$  and particulate  $\text{pNH}_4^+$  and  $\text{pNO}_3^-$  was of  $5.00 \pm 1.35$ ,  $1.34 \pm 0.23$ ,  $2.32 \pm 1.03$ ,  $1.64 \pm 0.34$ , and  $0.56 \pm 0.13 \text{ kg N ha}^{-1}$ , respectively. The annual total dry deposition of Nr during the 10-year period at this sampling site varied from  $6.96$  to  $13.1 \text{ kg N ha}^{-1}$  and the mean value was of  $10.5 \pm 1.83 \text{ kg N ha}^{-1}$  (Figure 4). The analysis of interannual variation showed that the total dry deposition of Nr decreased, with an average decrease of 39.4% by 2020 compared to 2011 (Figure 4).

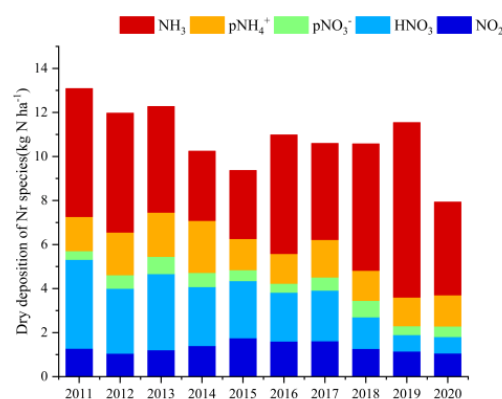


**Figure 4.** Distribution of the components of dry deposition of Nr components during 2011–2020.

### 3.4. Changes in Inorganic N Concentrations in Precipitation and Wet/Bulk N Deposition

Precipitation is generally high at this typical site in southern China. Annual precipitation varied from  $753$  to  $1608 \text{ mm}$  over the 10-year period, with a mean value of  $1410 \pm 296 \text{ mm}$  (Table 1). The annual mean concentrations of  $\text{NH}_4^+\text{-N}$  and  $\text{NO}_3^-\text{-N}$  in precipitation were mainly in the ranges of  $0.88\text{--}1.61$  and  $0.63\text{--}1.27 \text{ mg N L}^{-1}$ , and their

mean values were  $1.30 \pm 0.25$ , and  $0.97 \pm 1.85$  mg N L<sup>-1</sup>, respectively (Figure 5a). NH<sub>4</sub><sup>+</sup>-N dominated but declined: despite some fluctuations, the NH<sub>4</sub><sup>+</sup>-N concentration in precipitation in 2020 was 21.0% lower than that in 2011. The annual mean concentration of NO<sub>3</sub><sup>-</sup>-N also decreased by 28.8% in 2020 compared to 2011.

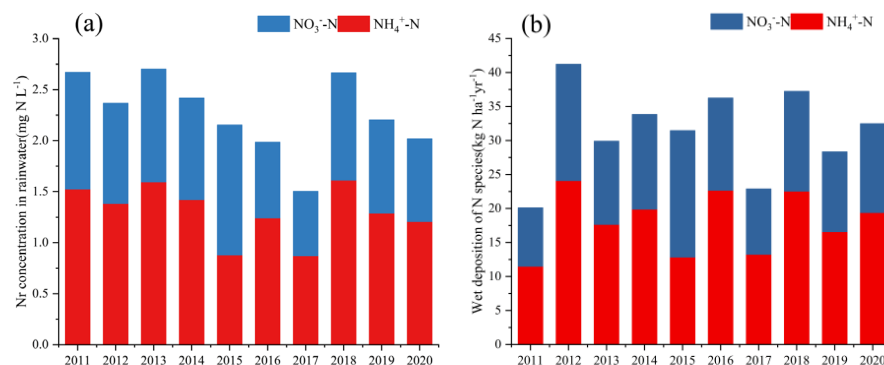


**Figure 5.** Distribution of annual average Nr concentrations (a) in rainwater and (b) wet/bulk N deposition from 2011–2020.

The annual mean wet/bulk deposition of NH<sub>4</sub><sup>+</sup>-N, NO<sub>3</sub><sup>-</sup>-N, and total inorganic N was in the ranges of 11.50–24.10, 8.61–18.61, and 20.11–37.24 kg N ha<sup>-1</sup>, respectively, with average values of  $18.04 \pm 4.2$ ,  $13.33 \pm 2.90$ , and  $31.37$  kg N ha<sup>-1</sup>, respectively (Figure 5b). The annual mean total wet/bulk deposition peaked in 2012 and declined gradually during the 10-year sampling period (without a statistically significant decreasing trend) (Figure 5b). Combining the analysis of reduced and oxidized N, NH<sub>4</sub><sup>+</sup>-N and NO<sub>3</sub><sup>-</sup>-N accounted for 58% and 42% of the wet/bulk deposition, respectively, suggesting that the former dominated. The correlation between precipitation and atmospheric inorganic N (NH<sub>4</sub><sup>+</sup>-N and NO<sub>3</sub><sup>-</sup>-N) concentrations, as important components of wet/bulk N deposition, was investigated. We found a negative logarithmic relationship between monthly mean inorganic N concentrations and monthly precipitation over the 10-year period (Figure 6).

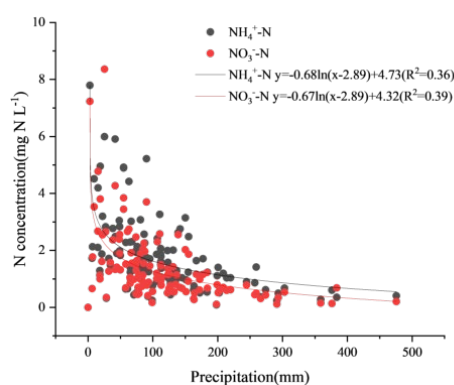


**Figure 6.** Monthly average concentrations of NH<sub>4</sub><sup>+</sup>-N and NO<sub>3</sub><sup>-</sup>-N in precipitation as a function of monthly average precipitation for the period 2011–2020.

### 3.5. Interannual Variation in Total Nitrogen Deposition

Total N deposition varied from 33.2 to 53.2 kg N ha<sup>-1</sup> yr<sup>-1</sup> and averaged  $41.9 \pm 6.0$  kg N ha<sup>-1</sup> yr<sup>-1</sup> over the 10-year period. The range of interannual variation was small and decreased by 24.0% in 2020 compared with the maximum value in 2012. The contributions of the components of dry deposition, i.e., gaseous NH<sub>3</sub>, NO<sub>2</sub>, and HNO<sub>3</sub>, plus particulate pNH<sub>4</sub><sup>+</sup> and pNO<sub>3</sub><sup>-</sup> to the mean annual deposition, were of 11.8%, 3.2%, 5.5%, 3.9%, and 1.3%, respectively; and those of the components of wet/bulk deposition, i.e., NH<sub>4</sub><sup>+</sup>-N and NO<sub>3</sub><sup>-</sup>-N to the mean annual deposition, were of 42.7% and 31.6%, respectively (Figure 7). Compared with dry deposition, wet/bulk deposition dominated the total N

deposition. Reduced N ( $\text{pNH}_4^+$  and  $\text{NH}_4^+\text{-N}$  in precipitation) contributed 58.4% to the total N deposition and oxidized N ( $\text{NO}_2$ ,  $\text{HNO}_3$ ,  $\text{pNO}_3^-$ , and  $\text{NO}_3^-\text{-N}$  in precipitation) accounted for 41.6%. Combined with the analysis in Sections 3.3 and 3.4, it can be seen that the contribution of reduced N to N deposition is greater than that of oxidized N, i.e., the key to controlling N deposition in rural areas of the south of China lies in controlling the emission of  $\text{NH}_3$ .

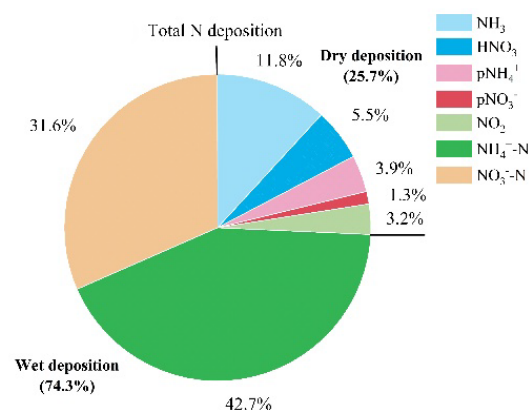


**Figure 7.** Contribution of components of wet and dry N deposition to total N deposition during 2011–2020.

## 4. Discussion

### 4.1. Changes in Atmospheric Reactive N Components

China's rapid agricultural development in the 21st century has caused significant environmental problems, such as severe air pollution and harmed human health [2,19]. Nr significantly contributes to  $\text{PM}_{2.5}$  [13]. In order to mitigate air pollution, during the 10-year period of this study, the Chinese government gradually improved the legislative mechanism for environmental protection and adopted a series of measures for environmental pollution control. Since the implementation of the national action plan for the prevention and control of air pollution (initiated in 2013), China's national air quality has improved. Significant reductions in  $\text{SO}_2$  and Nr emissions [20] and  $\text{PM}_{2.5}$  concentrations [21,22] have been reported:  $\text{PM}_{2.5}$  concentrations decreased at a rate of 9.1% per year and the number of days with  $\text{PM}_{2.5}$  concentrations higher than  $50 \mu\text{g m}^{-3}$  decreased from 2015 to 2018 [23], and those of  $\text{SO}_2$ ,  $\text{NO}_x$ , and  $\text{NH}_3$  decreased over 2015–2019. Overall, anthropogenic emissions of  $\text{SO}_2$ ,  $\text{NO}_x$ ,  $\text{NH}_3$ ,  $\text{PM}_{10}$ , and  $\text{PM}_{2.5}$  were estimated to have decreased by 53%, 20%, 10%, 21%, and 16%, respectively [24]. This trend was also reflected in southern China: from 2013 to 2015,  $\text{pNO}_3^-$  decreased significantly in the Pearl River Delta, Sichuan Basin, and Qinghai–Tibet Plateau [25], and  $\text{NO}_x$  emissions in the Pearl River Delta decreased by 27% [26]; from 2017 to 2020, the annual deposition of  $\text{NH}_4^+\text{-N}$  and  $\text{NO}_3^-\text{-N}$  in the Danjiangkou Reservoir area decreased, and the monthly dry deposition of  $\text{NO}_3^-\text{-N}$  significantly decreased ( $p < 0.01$ ) [27].

The effective control of agricultural activities can reduce N deposition. In recent years, farmers in Taojiang County, Hunan Province, have been asked to change crop rotations and to use available manure to replace some chemical fertilizers. This has led to an increase in nitrogen use efficiency (NUE) [13]. This, together with the gradual implementation of coal-to-gas conversion for heating in rural households, can reduce atmospheric Nr concentrations [28]. Our results show that the annual mean atmospheric  $\text{NO}_2$  and  $\text{HNO}_3$  concentrations decreased by 29.2% and 74.6% in 2020 compared to 2011. The annual mean  $\text{pNO}_3^-$  concentration remained low but also decreased during 2013–2016 and 2018–2020, with average decreases of 12.6% and 23.6%, respectively. The annual mean  $\text{pNH}_4^+$  concentration fluctuated during the 10-year period and increased by 26.29% in 2020 compared with 2011, which is worrying. However, overall, the atmospheric reactive N concentration and deposition in rural areas of southern China decreased from 2011 to

2020, indicating that the implementation of air pollution control measures were effective in decreasing N deposition and improving air quality in these regions. To further control particulate matter pollution in rural and urban areas, real-time monitoring and collaborative control of particulate matter and its precursor (e.g.,  $\text{NH}_3$  and  $\text{NO}_x$ ) emissions in rural areas should be strengthened.

#### 4.2. Changes in Atmospheric N Deposition and Its Ecological Effects

China is a world hotspot for atmospheric N deposition due to its rapid industrialization and intensive agricultural production [29]. The country's overall level of N deposition increased from the 1980s to the 2000s [2] but stabilized after the 2000s [30], mainly due to high emissions of  $\text{NH}_3$  and  $\text{NO}_x$  [14]. The south of China is densely populated with a well-developed agriculture, with consequent high  $\text{Nr}$  concentrations and high N deposition [17]. As strict air pollution control measures began to be implemented nationwide in 2013, N deposition in the south decreased [20]. Taojiang County, a key agricultural area in the south, suffered from high atmospheric  $\text{Nr}$  concentrations and dry N deposition during 2011–2013 (Figures 2 and 4) but, following the air pollution control actions introduced in 2013, the concentrations of many  $\text{Nr}$  species and dry N deposition began to decrease (see Section 4.1 for details); concentrations of N in wet/bulk N deposition also decreased to some extent [27]. We measured significant decreases in  $\text{NH}_4^+$ -N and  $\text{NO}_3^-$ -N concentrations in wet/bulk N deposition, with annual average concentrations in 2020 of 21.0% and 28.8%, respectively, compared with those in 2011. The concentration of inorganic N in precipitation at our site was lower than that in the northern region, and lower than the national average concentration of inorganic N in precipitation measured in China's Nationwide Nitrogen Deposition Monitoring Network [31]. Air pollution control has clearly played a positive role in reducing N deposition in Taojiang County, Hunan, southern China.

However, nitrogen supply could have positive effect too, together with drought periods occurring more frequently and higher  $\text{CO}_2$  levels in the air, which are helping the plants (trees) to cope with such climatic conditions [32]. Although the concentration of inorganic N in wet/bulk deposition decreased, the higher annual precipitation resulted in higher wet/bulk N deposition at our site. The annual average  $\text{NH}_4^+$ -N and  $\text{NO}_3^-$ -N deposition in wet/bulk deposition was up to  $31.4 \text{ kg N ha}^{-1}$  (Figure 6), which is higher than in other southern regions ( $21.1 \text{ kg N ha}^{-1} \text{ yr}^{-1}$ ) [33]. It is important to note that the main drivers of increased wet/bulk N deposition in China are increased energy consumption and N fertilizer use [34]. The ratio of  $\text{NH}_4^+$ -N to  $\text{NO}_3^-$ -N in wet deposition in this study was 1.35, which is slightly higher than the national average [35], indicating that agricultural activities are the main source of wet/bulk deposition.

Reductions in atmospheric N deposition in rural areas following government control of  $\text{Nr}$  emissions have been demonstrated in several developed countries and regions of the world: the range of total N deposition in rural Canada from 2000 to 2018 was between  $1.7$  and  $9.5 \text{ kg N ha}^{-1} \text{ yr}^{-1}$  [36]; and in 2018, N deposition on all land types in Europe declined to  $6.6 \text{ kg N ha}^{-1} \text{ yr}^{-1}$  [37,38]. As in other parts of the world,  $\text{Nr}$  emissions and deposition have decreased in China in recent years [39]. Our results show that the total  $\text{Nr}$  deposition in southern China during the last 10 years decreased, with less interannual variation, and with the total annual deposition varying from  $33.2$  to  $53.2 \text{ kg N ha}^{-1} \text{ yr}^{-1}$  with a mean value of  $41.9 \pm 6.0 \text{ kg N ha}^{-1} \text{ yr}^{-1}$ . This is higher than the national average ( $20.4 \pm 2.6 \text{ kg N ha}^{-1}$ ) [30,33], and much higher than that in developed regions of the world as represented by Europe and Canada, and exceeding the critical load for the sustainability of forest and grassland ecosystems [40].

From the perspective of specific components,  $\text{NH}_4^+$ -N contributed most to wet deposition and total N deposition, by 57.5% and 42.7%, respectively, and gaseous  $\text{NH}_3$  accounted for the largest proportion of dry deposition, at 46%. Overall, reduced N, including particulate  $\text{pNH}_4^+$ , contributed as much as 58.4% to the total N deposition. The annual mean reduced to oxidized N ratio in southern China varied from 0.7 to 1.6 during 2011–2020, with a mean of  $1.44 \pm 0.28$ , which is close to the national average of 1.7 in China [30]. Overall,

reduced-state N dominated, reflecting the fact that agricultural and non-agricultural  $\text{NH}_3$  in southern China jointly contribute to the total N deposition [41,42]:  $\text{NH}_x$  accounted for 61.2% and 57.5% of wet and dry deposition, respectively. This represents the increased importance of reduced N deposition compared to oxidized N deposition since the vigorous national control of  $\text{NO}_x$  emissions after 2010 [14].

Our results show that the strict implementation of air pollution control measures can reduce the concentrations of  $\text{Nr}$  in the atmosphere and reduce N deposition, improving China's air quality, ecosystems, and human health [19]. However, rural areas in southern China still need to adopt more comprehensive N deposition control measures in the context of environmental sustainability, food security, and human health [43], focusing on ammonia emission reduction, as well as source identification, prevention, and control.

## 5. Conclusions

This study of atmospheric  $\text{Nr}$  deposition at Taojiang, Hunan Province, for 10 consecutive years provides strong evidence for decreasing  $\text{Nr}$  concentrations, reducing atmospheric N deposition, and the improvement of air quality in southern China, but differently for the various components of  $\text{Nr}$ . Compared with 2011, atmospheric  $\text{HNO}_3$  concentrations in 2020 decreased by 74.6%;  $\text{NO}_2$  concentrations decreased by 29.2%; and  $\text{NH}_3$  concentrations decreased by 34.5%; however, concentrations of  $\text{pNH}_4^+$  and  $\text{pNO}_3^-$  increased by 26.3% and 70.8%. This reflects the complicated transformation mechanisms of atmospheric  $\text{Nr}$  into secondary particulate matter. Atmospheric  $\text{NH}_x$  concentrations stabilized after a peak in 2019, and  $\text{NO}_y$  concentrations decreased significantly after 2018 and again in 2020, with the effect of the COVID-19 epidemic being significant in that year. Dry N deposition in rural areas of southern China decreased by more than 30% over the 10-year period, and the total N deposition decreased by 24.0% in 2020 compared to the peak year. The data provide important evidence for the positive impact of air pollution control measures on air quality and atmospheric N deposition in the south of China. However, considering that  $\text{Nr}$  emissions and N deposition loads are still high, further emission control measures are needed to achieve air quality objectives, especially the urgent need to control  $\text{NH}_3$  emissions and thus particulate matter pollution by improving fertilizer use efficiency and livestock production.

**Author Contributions:** Conceptualization, X.L.; methodology, Z.W., W.X. and A.T.; software, K.R. and Y.Z.; validation, J.S.; formal analysis, K.R., Y.Z., Z.W. and J.L.; investigation, R.S., X.M., J.L., Y.Z. and Z.Y.; resources, X.L.; data curation, J.L., K.R. and Z.W.; writing—original draft preparation, K.R., Y.Z. and J.L.; writing—review and editing, X.L., Y.Z. and K.G.; visualization, X.L.; supervision, X.L. and A.T.; project administration, X.L.; funding acquisition, X.L. All authors have read and agreed to the published version of the manuscript.

**Funding:** This research was funded by the National Natural Science Foundation of China (42277097, 41425007), the Chinese State Key Special Program on Severe Air Pollution Mitigation “Agricultural Emission Status and Enhanced Control Plan” (DQGG0208), and the High-level Team Project of China Agricultural University.

**Institutional Review Board Statement:** Not applicable.

**Informed Consent Statement:** Not applicable.

**Data Availability Statement:** All data are available by contacting the corresponding author due to privacy reasons.

**Conflicts of Interest:** The authors declare no conflict of interest.

## References

1. Fowler, D.; Steadman, C.E.; Stevenson, D.; Coyle, M.; Rees, R.M.; Skiba, U.M.; Sutton, M.A.; Cape, J.N.; Dore, A.J.; Vieno, M.; et al. Effects of global change during the 21st century on the nitrogen cycle. *Atmos. Chem. Phys.* **2015**, *15*, 13849–13893. [[CrossRef](#)]
2. Liu, X.; Zhang, Y.; Han, W.; Tang, A.; Shen, J.; Cui, Z.; Vitousek, P.; Erisman, J.W.; Goulding, K.; Christie, P.; et al. Enhanced nitrogen deposition over China. *Nature* **2013**, *494*, 459–462. [[CrossRef](#)] [[PubMed](#)]

3. Galloway, J.N.; Townsend, A.R.; Erismann, J.W.; Bekunda, M.; Cai, Z.; Freney, J.R.; Martinelli, L.A.; Seitzinger, S.P.; Sutton, M.A. Transformation of the nitrogen cycle: Recent trends, questions, and potential solutions. *Science* **2008**, *320*, 889–892. [[CrossRef](#)] [[PubMed](#)]
4. Pan, Y.; Tian, S.; Liu, D.; Fang, Y.; Zhu, X.; Zhang, Q.; Zheng, B.; Michalski, G.; Wang, Y. Fossil fuel combustion-related emissions dominate atmospheric ammonia sources during severe haze episodes: Evidence from <sup>15</sup>N-stable isotope in size-resolved aerosol ammonium. *Environ. Sci. Technol.* **2016**, *50*, 8049–8056. [[CrossRef](#)] [[PubMed](#)]
5. Zhang, Y.; Benedict, K.B.; Tang, A.; Sun, Y.; Fang, Y.; Liu, X. Persistent nonagricultural and periodic agricultural emissions dominate sources of ammonia in urban Beijing: Evidence from <sup>15</sup>N stable isotope in vertical profiles. *Environ. Sci. Technol.* **2020**, *54*, 102–109. [[CrossRef](#)] [[PubMed](#)]
6. Feng, S.; Xu, W.; Cheng, M.; Ma, Y.; Wu, L.; Kang, J.; Wang, K.; Tang, A.; Collett, J.L., Jr.; Fang, Y.; et al. Overlooked Nonagricultural and wintertime agricultural NH<sub>3</sub> emissions in Quzhou county, North China Plain: Evidence from <sup>15</sup>N-stable isotopes. *Environ. Sci. Technol. Lett.* **2022**, *9*, 127–133. [[CrossRef](#)]
7. Suarez-Bertoa, R.; Zardini, A.; Astorga, C. Ammonia exhaust emissions from spark ignition vehicles over the new European driving cycle. *Atmos. Environ.* **2014**, *97*, 43–53. [[CrossRef](#)]
8. Lee, H.M.; Paulot, F.; Henze, D.K.; Travis, K.; Jacob, D.J.; Pardo, L.H.; Schichtel, B.A. Sources of nitrogen deposition in Federal Class I areas in the US. *Atmos. Chem. Phys.* **2016**, *16*, 525–540. [[CrossRef](#)]
9. Niemann, V.A.; Benedek, P.; Guo, J.; Xu, Y.; Blair, S.J.; Corson, E.R.; Nielander, A.C.; Jaramillo, T.F.; Tarpeh, W.A. Co-designing electrocatalytic systems with separations to improve the sustainability of reactive nitrogen management. *ACS Catal.* **2023**, *13*, 6268–6279. [[CrossRef](#)]
10. Clark, C.M.; Tilman, D. Loss of plant species after chronic low-level nitrogen deposition to prairie grasslands. *Nature* **2008**, *451*, 712–715. [[CrossRef](#)]
11. Zhan, X.; Bo, Y.; Zhou, F.; Liu, X.; Paerl, H.W.; Shen, J.; Wang, R.; Li, F.; Tao, S.; Dong, Y.; et al. Evidence for the importance of atmospheric nitrogen deposition to eutrophic Lake Dianchi, China. *Environ. Sci. Technol.* **2017**, *51*, 6699–6708. [[CrossRef](#)] [[PubMed](#)]
12. Chen, X.; Wang, Y.-H.; Ye, C.; Zhou, W.; Cai, Z.-C.; Yang, H.; Han, X. Atmospheric nitrogen deposition associated with the eutrophication of Taihu Lake. *J. Chem.* **2018**, *2018*, 4017107. [[CrossRef](#)]
13. Liu, X.; Xu, W.; Sha, Z.; Zhang, Y.; Wen, Z.; Wang, J.; Zhang, F.; Goulding, K. A green eco-environment for sustainable development: Framework and action. *Front. Agric. Sci. Eng.* **2020**, *7*, 67–74. [[CrossRef](#)]
14. Wen, Z.; Xu, W.; Li, Q.; Han, M.; Tang, A.; Zhang, Y.; Luo, X.; Shen, J.; Wang, W.; Li, K.; et al. Changes of nitrogen deposition in China from 1980 to 2018. *Environ. Int.* **2020**, *144*, 106022. [[CrossRef](#)] [[PubMed](#)]
15. Luo, X.; Liu, X.; Pan, Y.; Wen, Z.; Xu, W.; Zhang, L.; Kou, C.; Lv, J.; Goulding, K. Atmospheric reactive nitrogen concentration and deposition trends from 2011 to 2018 at an urban site in north China. *Atmos. Environ.* **2020**, *224*, 117298. [[CrossRef](#)]
16. Fu, Y.; Xu, W.; Wen, Z.; Han, M.; Sun, J.; Tang, A.; Liu, X. Enhanced atmospheric nitrogen deposition at a rural site in northwest China from 2011 to 2018. *Atmos. Res.* **2020**, *245*, 105071. [[CrossRef](#)]
17. Zhu, X.; Shen, J.; Li, Y.; Liu, X.; Xu, W.; Zhou, F.; Wang, J.; Reis, S.; Wu, J. Nitrogen emission and deposition budget in an agricultural catchment in subtropical central China. *Environ. Pollut.* **2021**, *289*, 117870. [[CrossRef](#)]
18. Bai, Z.; Fan, X.; Jin, X.; Zhao, Z.; Wu, Y.; Oenema, O.; Velthof, G.; Hu, C.; Ma, L. Relocate 10 billion livestock to reduce harmful nitrogen pollution exposure for 90% of China's population. *Nat. Food* **2022**, *3*, 152–160. [[CrossRef](#)]
19. Gao, C.; Liu, M. The impact of local environment and neighboring pollution on the spatial variation of particulate matter in Chinese mainland. *Atmosphere* **2023**, *14*, 186. [[CrossRef](#)]
20. Jiang, W.; Shen, J.; Li, Y.; Wang, J.; Gong, D.; Zhu, X.; Liu, X.; Liu, J.; Reis, S.; Zhu, Q.; et al. Contrasting change trends in dry and wet nitrogen depositions during 2010 to 2020: Evidence from an agricultural catchment in subtropical Central China. *Sci. Total Environ.* **2023**, *907*, 168094. [[CrossRef](#)]
21. Dai, T.; Cheng, Y.; Goto, D.; Li, Y.; Tang, X.; Shi, G.; Nakajima, T. Revealing the sulfur dioxide emission reductions in China by assimilating surface observations in WRF-Chem. *Atmos. Chem. Phys.* **2021**, *21*, 4357–4379. [[CrossRef](#)]
22. Kan, X.; Liu, X.; Zhou, Z.; Zhang, Y.; Zhu, L.; Sian, K.T.C.L.K.; Liu, Q. Analysis of spatiotemporal variation and influencing factors of PM<sub>2.5</sub> in China based on multisource data. *Sustainability* **2023**, *15*, 14656. [[CrossRef](#)]
23. Zhong, Q.; Tao, S.; Ma, J.; Liu, J.; Shen, H.; Shen, G.; Guan, D.; Yun, X.; Meng, W.; Yu, Y.; et al. PM<sub>2.5</sub> reductions in Chinese cities from 2013 to 2019 remain significant despite the inflating effects of meteorological conditions. *One Earth* **2021**, *4*, 448–458. [[CrossRef](#)]
24. Gu, C.; Zhang, L.; Xu, Z.; Xia, S.; Wang, Y.; Li, L.; Wang, Z.; Zhao, Q.; Wang, H.; Zhao, Y. High-resolution regional emission inventory contributes to the evaluation of policy effectiveness: A case study in Jiangsu Province, China. *Atmos. Chem. Phys.* **2023**, *23*, 4247–4269. [[CrossRef](#)]
25. Li, R.; Cui, L.; Zhao, Y.; Zhou, W.; Fu, H. Long-term trends of ambient nitrate (NO<sub>3</sub><sup>-</sup>) concentrations across China based on ensemble machine-learning models. *Earth Syst. Sci. Data* **2021**, *13*, 2147–2163. [[CrossRef](#)]
26. Zhong, B.; Wang, X.; Ye, L.; Ma, M.; Jia, S.; Chen, W.; Yan, F.; Wen, Z.; Padmaja, K. Meteorological variations impeded the benefits of recent NO<sub>x</sub> mitigation in reducing atmospheric nitrate deposition in the Pearl River Delta region, Southeast China. *Environ. Pollut.* **2020**, *266*, 115076. [[CrossRef](#)]

27. Guo, X.; Zhang, Q.; Zhao, T.; Jin, C. Fluxes, characteristics and influence on the aquatic environment of inorganic nitrogen deposition in the Danjiangkou reservoir. *Ecotoxicol. Environ. Saf.* **2022**, *241*, 113814. [[CrossRef](#)] [[PubMed](#)]
28. Zhao, N.; Li, B.; Li, H.; Ahmad, R.; Peng, K.; Chen, D.; Yu, X.; Zhou, Y.; Dong, R.; Wang, H.; et al. Field-based measurements of natural gas burning in domestic wall-mounted gas stove and estimates of climate, health and economic benefits in rural Baoding and Langfang regions of Northern China. *Atmos. Environ.* **2020**, *229*, 117454. [[CrossRef](#)]
29. Zhu, H.; Chen, Y.; Zhao, Y.; Zhang, L.; Zhang, X.; Zheng, B.; Liu, L.; Pan, Y.; Xu, W.; Liu, X. The response of nitrogen deposition in China to recent and future changes in anthropogenic emissions. *J. Geophys. Res. Atmos.* **2022**, *127*, e2022JD037437. [[CrossRef](#)]
30. Chen, S.; Chen, B.; Wang, S.; Sun, L.; Shi, H.; Liu, Z.; Wang, Q.; Li, H.; Zhu, T.; Li, D.; et al. Spatiotemporal variations of atmospheric nitrogen deposition in China during 2008–2020. *Atmos. Environ.* **2023**, *315*, 120120. [[CrossRef](#)]
31. Xu, W.; Luo, X.S.; Pan, Y.P.; Zhang, L.; Tang, A.H.; Shen, J.L.; Zhang, Y.; Li, K.H.; Wu, Q.H.; Yang, D.W.; et al. Quantifying atmospheric nitrogen deposition through a nationwide monitoring network across China. *Atmos. Chem. Phys.* **2015**, *15*, 12345–12360. [[CrossRef](#)]
32. Ofori-Amanfo, K.K.; Klem, K.; Veselá, B.; Holub, P.; Agyei, T.; Juráň, S.; Grace, J.; Marek, M.V.; Urban, O. The effect of elevated CO<sub>2</sub> on photosynthesis is modulated by nitrogen supply and reduced water availability in *Picea abies*. *Tree Physiol.* **2023**, *43*, 925–937. [[CrossRef](#)] [[PubMed](#)]
33. Xu, W.; Liu, L.; Cheng, M.; Zhao, Y.; Zhang, L.; Pan, Y.; Zhang, X.; Gu, B.; Li, Y.; Zhang, X.; et al. Spatial–temporal patterns of inorganic nitrogen air concentrations and deposition in eastern China. *Atmos. Chem. Phys.* **2018**, *18*, 10931–10954. [[CrossRef](#)]
34. Jia, Y.; Yu, G.; He, N.; Zhan, X.; Fang, H.; Sheng, W.; Zuo, Y.; Zhang, D.; Wang, Q. Spatial and decadal variations in inorganic nitrogen wet deposition in China induced by human activity. *Sci. Rep.* **2014**, *4*, 3763. [[CrossRef](#)] [[PubMed](#)]
35. Zhu, J.; He, N.; Wang, Q.; Yuan, G.; Wen, D.; Yu, G.; Jia, Y. The composition, spatial patterns, and influencing factors of atmospheric wet nitrogen deposition in Chinese terrestrial ecosystems. *Sci. Total Environ.* **2015**, *511*, 777–785. [[CrossRef](#)] [[PubMed](#)]
36. Cheng, I.; Zhang, L.; He, Z.; Cathcart, H.; Houle, D.; Cole, A.; Feng, J.; O'Brien, J.; Macdonald, A.M.; Aherne, J.; et al. Long-term declines in atmospheric nitrogen and sulfur deposition reduce critical loads exceedances at multiple Canadian rural sites, 2000–2018. *Atmos. Chem. Phys.* **2022**, *22*, 14631–14656. [[CrossRef](#)]
37. Engardt, M.; Simpson, D.; Schwikowski, M.; Granat, L. Deposition of sulphur and nitrogen in Europe 1900–2050. Model calculations and comparison to historical observations. *Tellus B Chem. Phys. Meteorol.* **2017**, *69*, 1328945. [[CrossRef](#)]
38. Schmitz, A.; Sanders, T.G.M.; Bolte, A.; Bussotti, F.; Dirnböck, T.; Johnson, J.; Peñuelas, J.; Pollastrini, M.; Prescher, A.-K.; Sardans, J.; et al. Responses of forest ecosystems in Europe to decreasing nitrogen deposition. *Environ. Pollut.* **2019**, *244*, 980–994. [[CrossRef](#)] [[PubMed](#)]
39. Xie, D.; Zhang, T.; Yu, Q.; Huang, Y.; Mulder, J.; Duan, L. A sharp decline in nitrogen input in a N-saturated subtropical forest causes an instantaneous reduction in nitrogen leaching. *J. Geophys. Res. Biogeosci.* **2018**, *123*, 3320–3330. [[CrossRef](#)]
40. Bobbink, R.; Hicks, K.; Galloway, J.; Spranger, T.; Alkemade, R.; Ashmore, M.; Bustamante, M.; Cinderby, S.; Davidson, E.; Dentener, F.; et al. Global assessment of nitrogen deposition effects on terrestrial plant diversity: A synthesis. *Ecol. Appl.* **2010**, *20*, 30–59. [[CrossRef](#)]
41. Wang, H.; Yang, F.; Shi, G.; Tian, M.; Zhang, L.; Zhang, L.; Fu, C. Ambient concentration and dry deposition of major inorganic nitrogen species at two urban sites in Sichuan Basin, China. *Environ. Pollut.* **2016**, *219*, 235–244. [[CrossRef](#)] [[PubMed](#)]
42. Gu, B.; Sutton, M.A.; Chang, S.X.; Ge, Y.; Chang, J. Agricultural ammonia emissions contribute to China's urban air pollution. *Front. Ecol. Environ.* **2014**, *12*, 265–266. [[CrossRef](#)]
43. Guo, Y.; Chen, Y.; Searchinger, T.D.; Zhou, M.; Pan, D.; Yang, J.; Wu, L.; Cui, C.; Zhang, W.; Zhang, F.; et al. Air quality, nitrogen use efficiency and food security in China are improved by cost-effective agricultural nitrogen management. *Nat. Food* **2020**, *1*, 648–658. [[CrossRef](#)] [[PubMed](#)]

**Disclaimer/Publisher's Note:** The statements, opinions and data contained in all publications are solely those of the individual author(s) and contributor(s) and not of MDPI and/or the editor(s). MDPI and/or the editor(s) disclaim responsibility for any injury to people or property resulting from any ideas, methods, instructions or products referred to in the content.